Comparison of Narrow-Band OFDM PLC Solutions and I-UWB Modulation over Distribution Grids

Andrea M. Tonello*, Salvatore D'Alessandro*, Fabio Versolatto*, and Carlo Tornelli†
* DIEGM - Università di Udine - Via delle Scienze 208 - 33100 Udine - Italy
e-mail: {tonello, salvatore.dalessandro, fabio.versolatto}@uniud.it
† RSE SpA - Via Rubattino 54 - 20143 Milano - Italy
e-mail: carlo.tornelli@rse-web.it

***Abstract*—To support the requirements of smart grids (SGs) applications, telecommunication industries and standardization organizations have proposed to use narrow-band (NB) orthogonal frequency division multiplexing (OFDM) based solutions over power line communications (PLCs) networks. Among these solutions, the most important are the PoweRline Intelligent Metering Evolution (PRIME), the ERDF G3-PLC, and the G3-FCC.**

Impulsive-ultrawide band (I-UWB) is a broadband modulation technique which has recently been proposed for robust low rate command and control applications over MV and outdoor-low voltage (O-LV) channels.

In this paper, we compare the performances of G3-PLC, PRIME, G3-FCC, and I-UWB solutions in terms of capacity and power consumption when transmission is over distribution networks.

Through numerical results, we have found that in most cases, on equal transmitted power, I-UWB shows much higher capacity values than NB-OFDM based solutions. The capacity gains directly translate in power savings, and range extensions when we impose the target rate of I-UWB to be equal to the capacity of NB-OFDM based solutions. Therefore, I-UWB can be considered an alternative to more conventional NB OFDM solutions for SG applications.

I. Introduction

In the past years we have assisted to an increased interest of the utility companies toward the development of more or less sophisticated power line communication (PLC) technologies that allow the remote automatic meter management (AMM).

Besides the need of AMM technologies, nowadays the utility companies are facing new challenges such as [1]: the safe integration and the management of renewable energy sources; the management of plug-in electric vehicles that may cause a large load increase on sections of the grid; the management of demand side and demand response allowing the customers to collaborate in order to adapt the production and the delivery of electricity to achieve energy efficiency and saving.

Therefore, in the next years, the electricity grid will be viewed as a smart grid (SG), namely, a distributed complex large scale system that needs to smartly manage flows of electricity produced by big or small plants.

The management of the SG requires a pervasive telecommunication infrastructure that allows a bidirectional, reliable, short and long distance communication. Among the communication technologies, power line communications (PLCs) are best suited for SG applications. In fact, the PLC infrastructure is pervasively deployed and its exploitation for communication purposes does not require any additional cost.

The frequency bands dedicated from standardization organizations to narrow-band PLC devices useful for SG applications, vary among the continents. In the EU, the CENELEC issued the standard EN 50065 which specifies four frequency bands for communications over PL networks [1]. The band A (3-95 kHz) is reserved exclusively to power utilities. The band B (95-125 kHz) can be used for any application. The band C (125-140 kHz) is dedicated to in-home networking systems. The band D (140-148.5 kHz) is reserved to alarm and security systems. In the US and Asia, the regulation is different. FCC and ARIB allow PLC devices to work in the band 3-500 kHz.

The PLC devices that work in the frequency bands above specified are classified as narrow-band (NB) devices. This is to distinguish them from broadband (BB) devices that usually signal in the frequency band 2-30 MHz, and that are typically used for high rate in-home applications. Recently, BB PLC devices have also been proposed for "in-home" SG applications, e.g., the HomePlug Green Phy [2] that works in the 2-30 MHz band.

The NB PLC technologies that are adopted or are being developed for SG applications can be classified according to the modulation scheme used at the physical layer, i.e., single or multi-carrier.

The NB technologies based on single carrier modulation do not offer enough data rate as required by SG applications, e.g., the Italian utility ENEL has deployed smart metering devices which are based on single carrier frequency shift keying (FSK) modulation. They only allow the bimonthly remote reading of the power consumption.

To be able to support the requirements of the SG applications, industries and standardization organizations have proposed the use of NB multi-carrier solutions. The most important ones are the PoweRline Intelligent Metering Evolution

This work has been partly funded by the Research Fund for the Italian Electrical System under the Contract Agreement between RSE (formerly known as ERSE) and the Ministry of Economic Development - General Directorate for Nuclear Energy, Renewable Energy and Energy Efficiency stipulated on July 29, 2009 in compliance with the Decree of March 19, 2009.

(PRIME) [3], and the ERDF G3-PLC [4]. Both solutions are specified for working over low voltage (LV) networks in the CENELEC-A frequency band. Nevertheless, in [5] it has been shown that G3-PLC is able to work also over medium voltage (MV) lines. Recently, Maxim has proposed an extended version of the G3 solution that also works in the frequency band defined by FCC, i.e., G3-FCC [6]. It is interesting to note tha G3-FCC seems to serve as base technology for the development of the upcoming IEEE P1901.2 and ITU G.hnem SG standards [5].

At the physical layer, all the previous solutions adopt orthogonal frequency division multiplexing (OFDM). As it is well known, the attractive features of OFDM are: the use of a cyclic prefix (CP) to cope with the intersymbol interference caused by signaling over a dispersive channel; a simple one-tap sub-channel equalization; a good notching capability by switching off sub-channels which are dedicated to other telecommunication systems, e.g., AM radio; a good spectral efficiency thanks to the use of bit and power loading algorithms.

Recently, in [7] the authors investigated the use of impulsive-ultrawide band (I-UWB) modulation for robust low rate command and control applications over MV and outdoor-low voltage (O-LV) channels.

Basically, I-UWB is a BB solution which conveys data by mapping the information symbols into short pulses. In order to cope with the channel time dispersion, the pulses are followed by a guard time during which the transmitter is silent. The receiver is based on a matched filter concept [8]. Some of the advantages of using I-UWB w.r.t. OFDM are: a lower implementation complexity; the robustness against narrow-band interference; the capability of decoding a signal transmitted with a much smaller power.

In this paper, we compare the performances of G3-PLC, PRIME, G3-FCC, and I-UWB solutions in terms of capacity and power consumption when signaling over measured MV channels and O-LV channels, i.e., distribution networks. Through numerical results, we have found that, in most cases, I-UWB shows much higher capacity values than NB OFDM based solutions over both MV and LV channels on equal transmitted power. The capacity gains directly translate in power savings when imposing the target rate of I-UWB to be equal to the capacity of NB OFDM based solutions. Therefore, I-UWB can be considered an alternative to more conventional NB OFDM solutions for SG applications.

The paper is organized as follows. In Sections II and III, we describe the channel and the noise models. In Section IV, we briefly recall the NB OFDM based solutions and the I-UWB modulation. In Section V, we report the numerical results. Finally, the conclusions follow in Section VI.

II. Channel Models

We focus on two PLC application scenarios, namely, the outdoor low voltage and the medium voltage. The first accounts for communications between houses and the transformer stations. The latter focuses on the communications between different transformer stations through the MV lines. In this work we do not consider channels defined through the MV/LV transformers.

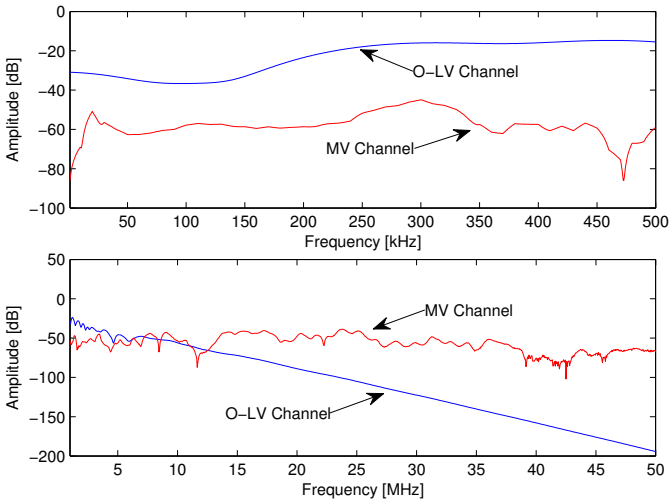

Fig. 1. An example of outdoor LV and MV channel frequency response in the narrow-band (top) and broadband (bottom) frequency range.

While for the O-LV scenario, the analytical expression of several reference channels has been provided in [9], for the MV scenario, no reference model has been provided yet. Therefore, we performed a measurement campaign on a real MV test network. We collected 42 channel responses and we used them for simulation purposes. In the following, we describe the O-LV reference channels of [9], the MV test network and the setup of the measurement campaign.

A. Outdoor-Low Voltage Channels

We exploit the channel models derived in [9] from the results of a measurement campaign. Basically, the measured channels are divided into three classes according to the length of the channel backbone, i.e., the shortest signal path between the transmitter and the receiver. For each class, up to three channels have been selected as representatives, and a total amount of eight reference channels is given. All the reference channels show a distinct low pass behaviour and the attenuation beyond 20 MHz is always greater than 50 dB. Furthermore, several channels exhibit strong frequency notches and long time dispersion. Namely, the duration of the impulse response is approximately between 1.5 and 10 μs.

The reference channels are described according to the multipath propagation model [10] and the values of the model parameters are given for all the channels. We exploit this analytical representation to extend the model up to 50 MHz. In Fig. 1, we show the amplitude of the frequency response of a reference channel. The channel is representative of an outdoor LV channel whose backbone length is approximately 150 m. As it can be noted, the attenuation strongly increases with the frequency and fading effects are concentrated in the lower frequency range.

B. Medium Voltage Channels

We performed a measurement campaign on a 20 kV medium voltage network that we described in [7]. The network feeds a large number of users concentrated in a small area. In detail, it is a three-phase network with four transformer stations and one independent MV switch. Several MV/LV transformers are connected to the network. The network is ring shaped, and the MV switch is left open. Therefore, the network has a tree structure without loops. Every station is connected to the two adjacent ones via underground MV cables. Both the ends of the MV cables terminate into a cable switch, inside the transformer station.

We used inductive couplers. We placed the couplers next to the cable switches, on a single phase of the MV cables. Therefore, we study channels where the transmitter and the receiver are connected to the same phase.

We collected 42 different channels. The measurements have been performed in the time domain and the results have validity up to 55 MHz. For the simulations, we consider the truncated impulse response of the channels that contains 95% of the channel energy. In Fig. 1, we provide an example of the frequency response of a MV channel. As shown in the figure, we have found that, in most of the cases, MV channels exhibit lower attenuations in the higher frequency range, w.r.t. to the O-LV channels.

III. Noise Models

We assume the noise to be stationary and we model it as additive colored Gaussian. We refer to the noise as background noise. In PLCs the background noise is colored, with a power spectral density (PSD) that decreases as the frequency increases. The lower frequency range, namely up to few MHz, experiences higher levels of man-made noise. Furthermore, in most of the cases, the decrease follows an exponential rule that converges to a noise floor in the higher frequency range. It has been shown that this behaviour is valid for all the PLC application scenarios, even though the noise floor level may vary.

In the literature, the measurement campaigns have turned out different models for the NB and the BB background noise. In the following, we describe the models that we adopt in this work.

A. Narrow-band

We model the NB (3-500 kHz) background noise according to the model described in [11]. Therein, the authors made a set of measurements over MV networks, and they found that the PSD of the colored background noise decreases exponentially as it is shown in Fig. 2. We notice that the exponential behaviour of the NB background noise has also been experienced in US distribution grids [5].

B. Broadband

We model the BB (2-50 MHz) background noise according to the models provided in [9]. In Fig. 2, we show the PSD models. The models have been derived from the results of measurement campaigns that have been performed in real networks. Measures have shown a high variability of the background noise PSD, and thus the models in [9] are expressed in terms of an average profile and a tolerance interval. In this work, we follow a conservative approach, i.e., we model the noise PSD according to the highest levels of measured noise.

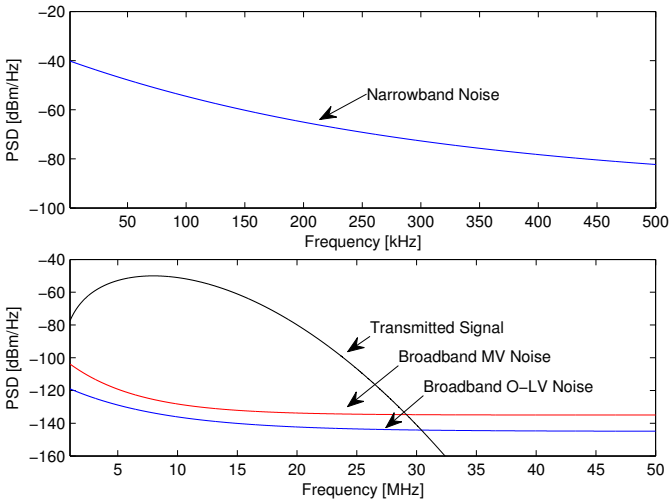

Fig. 2. PSD of the narrow-band noise model (top). PSD of the I-UWB transmitted signal, and of the outdoor LV and MV broadband noise models (bottom).

IV. Modulation Schemes

In this section we briefly recall the OFDM and the I-UWB modulation schemes. More precisely, in Sub-Section IV-A, we recall the basis of OFDM and we list the parameters used by PRIME, G3-PLC, and G3-FCC. Then, in Sub-Section IV-B, we focus on I-UWB.

A. OFDM

We consider an OFDM baseband system whose transmitter comprises the following steps. The low rate data symbols $b^{(k)}(\ell N)$, with $k = 0, \ldots, M-1$, and $N \geq M$ equal to the OFDM symbol duration in samples, are processed by an M-points inverse discrete Fourier transform (IDFT). The IDFT output is extended with a CP of μ samples. The signal is then transmitted over a dispersive channel whose duration equals ν samples.

The receiver consists of the following steps. We first acquire symbol synchronization. We then discard μ samples, and we apply an M-points DFT on the remaining M samples. Finally, we perform zero forcing single-tap sub-channel equalization.

Assuming Gaussian distributed data symbols, and stationary colored Gaussian noise, we can compute the capacity of the OFDM system as [12]:

$$C_{ofdm} = \frac{1}{(M+\mu)\,T} \sum_{k \in \mathbb{K}_{ON}} \log_2 \left(1 + \gamma_{ofdm}^{(k)}\right) \; [bit/s], \quad (1)$$

where T denotes the sampling factor, $\mathbb{K}_{ON}$ denotes the set of used sub-channels, i.e., $\mathbb{K}_{ON} \subseteq \{0, \ldots, M-1\}$, and $\gamma_{ofdm}^{(k)}$

TABLE I
OFDM SYSTEM PARAMETERS FOR PRIME, G3-PLC, AND G3-FCC.

	PRIME	G3-PLC	G3-FCC
1/T [kHz]	125	200	600
M	256	128	128
μT [μs]	192	75	75
cardinality of $\mathbb{K}_{ON}$	97	36	72
Start frequency [kHz]	41.9	35.9	45.3
Stop frequency [kHz]	88.8	90.6	478.1

denotes the signal to interference plus noise ratio (SINR) experienced in sub-channel k. It is defined as

$$\gamma_{ofdm}^{(k)} = \frac{P_{b,ofdm}^{(k)}|G^{(k)}|^2}{P_{I,ofdm}^{(k)} + P_{W,ofdm}^{(k)}}. \quad (2)$$

In (2), $P_{b,ofdm}^{(k)}$, $P_{I,ofdm}^{(k)}$, and $P_{W,ofdm}^{(k)}$ respectively denote the transmitted data symbol, the interference, and the noise power terms in sub-channel k. Furthermore, $G^{(k)}$ represents the amplitude of the data of interest in sub-channel k. Please, refer to [13] for details regarding the computation of the power terms.

As we can see from (2), the received signal can be affected by interference. It is well known that if the CP lasts more than the channel duration, i.e., $\mu \geq \nu - 1$ the received signal will be neither affected by inter-carrier interference (ICI) nor by inter symbol interference (ISI). Nevertheless, in the case that the CP is shorter than the channel duration, interference occurs.

As stated during the introduction, PRIME, G3-PLC, and G3-FCC solutions adopt OFDM as modulation scheme. More precisely, the PRIME solution adopts pure OFDM, whereas both G3-PLC and G3-FCC adopt pulse-shaped (PS)-OFDM. PS-OFDM is an OFDM where each OFDM symbol, before being transmitted, is windowed and overlapped with a part of the previous symbol [14, Section 5.3.2]. The advantage of using PS-OFDM is due to a better sub-channel frequency confinement w.r.t. OFDM. This characteristic is useful whenever frequency notching is required for coexistence purposes. In this work we do not consider the problem of notching and therefore we assume that all the considered NB-OFDM based solutions use pure OFDM.

In Table I, we report the OFDM parameters that will be used in Section V to compute the performances of PRIME [3], G3-PLC [4], and G3-FCC [6].

From Table I, we highlight that we use a CP of duration equal to 75 μs for G3-FCC, instead of the value of 25 μs as specified in [5], [6]. This is because we have numerically found that over the MV channels described in Section II that experience the noise described in Section III, the CP that maximizes the average capacity value of G3-FCC is equal to 75 μs. This value of CP also permits the system to behave good over LV channels.

Finally, when showing numerical results, we assume that the NB-OFDM systems have to satisfy a PSD mask constraint of [4] 120 dBμV/200Hz (-13 dBm/Hz). This is to be compliant with the electromagnetic compatibility directive. In such a case, it is possible to show that the sub-channels power allocation that maximizes the OFDM capacity corresponds with the one given by the same PSD constraint [15], and thus we equally distribute the power across the set $\mathbb{K}_{ON}$ at the level given by the PSD constraint.

B. I-UWB Modulation

The idea behind impulsive modulation is to map the information symbols into short duration pulses followed by a silent period, i.e., the guard time. We refer to the short duration pulse as monocycle and to the composition of a monocycle and the subsequent guard time as a frame. Therefore, the transmitter can be implemented with a simple pulser which transmits symbols with rate $1/T_f$, where T_f is the frame duration. If the guard time is sufficiently long, we do not experience ISI. In the following, we use $T_f = 5\,\mu s$ [7].

The shape of the monocycle determines the signalling bandwidth. We avoid transmissions in the lower frequency range, where we experience the highest levels of background noise and further, where we may interfere with narrow-band PLCs. Therefore, we shape the monocycle as the second derivative of the Gaussian pulse. In Fig. 2, we show the average PSD of the transmitted signal. We highlight that the PSD is not flat in a certain frequency interval. Hence, we conventionally define the signalling bandwidth B as the highest frequency beyond which the PSD of the transmitted signal falls 30 dB below its maximum. Further, we point out that increasing the signalling bandwidth, the maximum of the transmitted PSD moves toward the higher frequencies due to the shape of the monocycle. We choose $B = 20$ MHz. It follows that, according to FCC, the used modulation can be classified as ultra wide band because the ratio between the signalling bandwidth and the central frequency exceeds 0.2.

We assume the average power spectral density of the transmitted signal to be lower than PSD_{max}. Given PSD_{max}, the transmitted energy is a function of the signalling bandwidth. No form of notching is considered, and thus coexistence or norm limitations are satisfied by properly selecting the value of PSD_{max}. In particular, we are interested in coexistence with narrow-band PLC standards. We have found that, in the $0 - 500$ kHz frequency range, the average PSD of the transmitted signal is always 40 dB below PSD_{max}, when $B = 20$ MHz.

We assume a single link packet transmission and the receiver to be the optimal one. The optimal receiver is based on the matched filter concept. Basically, it correlates the received signal with a template waveform that is matched to the noise correlation and the channel [8]. The output is then sampled to obtain a scalar metric for each symbol/frame, namely, $\Lambda(\ell T_f)$.

In the following, we address the best attainable performances, and thus we assume perfect knowledge of the channel and the noise correlation at the receiver. Practical receiver algorithms have been proposed in [16]. We compute the SINR

TABLE II
CAPACITY IN THE MV SCENARIO.

	PRIME	G3-PLC	G3-FCC	I-UWB same power of G3-PLC	I-UWB same power of G3-FCC
min [kbps]	0.002	0.006	8.002	494.0	967.7
mean [kbps]	3.337	3.905	393.9	2148	2608
max [kbps]	55.52	41.20	1593	3959	4478

TABLE III
CAPACITY IN THE O-LV SCENARIO.

	PRIME	G3-PLC	G3-FCC	I-UWB same power of G3-PLC	I-UWB same power of G3-FCC
min [kbps]	0.584	1.978	1286	418	876.1
mean [kbps]	103.9	114.8	2295	1683	2143
max [kbps]	265.4	302.2	3373	3677	4178

from the samples of $\Lambda(\ell T_f)$. We define it as

$$\gamma_{i\text{-}uwb} = \frac{|g_{eq}(0)|^2 P_{b,i\text{-}uwb}}{P_I + P_W}\,, \tag{3}$$

where $g_{eq}(0)$, $P_{b,i\text{-}uwb}$, P_I and P_W are the equivalent channel amplitude, the transmitted data symbol[1] power and the power of the ISI and noise components of $\Lambda(\ell T_f)$, respectively. We define the equivalent channel impulse response as the convolution of the monocycle, the channel response and the matched filter impulse response. We further point out that P_I is a function of the transmitted signal power. More in detail, $P_I = k_I P_{b,i\text{-}uwb}$ with k_I being constant and a function of the equivalent channel response. Now, with the same assumptions of (1), we define the system capacity as

$$C_{i\text{-}uwb} = \frac{1}{T_f}\log_2\left(1+\gamma_{i\text{-}uwb}\right) \quad [bit/s]\,. \tag{4}$$

Furthermore, from (4), we can compute the power, and thus the average maximum PSD level, required by I-UWB to obtain a target rate value $\hat{C}$ as

$$P_{b,i\text{-}uwb} = \frac{\left(2^{\hat{C}T_f}-1\right)P_W}{|g_{eq}(0)|^2 - k_I\left(2^{\hat{C}T_f}-1\right)} \quad [W]\,. \tag{5}$$

In this respect, we point out that the target rate value $\hat{C}$ must be achievable in order to have $P_{b,i\text{-}uwb} \geq 0$.

Finally, we remark that we choose the value of the frame duration and the bandwidth that allow attaining the best performance in the MV scenario, according to the results in [7].

[1] $P_{b,i\text{-}uwb}$ represents the average statistical power of the transmitted signal under the assumption of a unitary energy pulse.

V. NUMERICAL RESULTS

In order to obtain numerical results for the NB OFDM based systems, we consider the parameters of Table I. Furthermore, we assume to transmit the OFDM signals with a PSD of [4] -13 dBm/Hz in the used frequency band which is defined by the set $\mathbb{K}_{ON}$ according to the specs.

From Section IV, we here recall that the PRIME and the G3-PLC solutions both work on the CENELEC A frequency band, whereas, the G3-FCC is specified for working on the FCC frequency band.

To compare the I-UWB system with the NB OFDM ones, we set its transmitted power, namely $P_{b,i\text{-}uwb}$, equal to that of the specific OFDM scheme under comparison.

In Table II, we list the minimum, the maximum, and the mean capacity values obtained using the PRIME, the G3-PLC, the G3-FCC, and the I-UWB systems over MV channels. In Table III, we report the same results for the outdoor LV channels.

From Tables II-III, we first notice that in average G3-PLC outperforms PRIME. For this reason we choose to set the power transmitted by I-UWB only equal to the one of G3-PLC when considering the comparison for the CENELEC A band, and equal to the one of G3-FCC for the FCC band. As a result, we have that the maximum level of PSD transmitted by I-UWB, namely PSD_{max} (see Section IV), is respectively equal to -34.03 and -26.18 dBm/Hz for the bands CENELEC A and FCC.

From Tables II-III, we also notice the followings.

- Over MV channels, both PRIME and G3-PLC are not reliable for smart grid applications inasmuch their minimum capacity value is of only some bps. Impressively, I-UWB allows for a minimum capacity value of 497 kbps although it transmits the same power of G3-PLC.
- All the NB OFDM based solutions work better over LV channels. This is because, considering the frequency band up to some MHz (see Fig. 1), the average MV channel attenuation is higher than the one of LV channels. Conversely, I-UWB works better over MV channels because the transmitted signal exploits the lower attenuation that we experience in the higher frequency range w.r.t. the O-LV scenario. This is mainly due to the shape of the monocycle.
- Over LV channels, G3-FCC is more reliable than I-UWB inasmuch its minimum and mean capacity values are higher than that of I-UWB, even though I-UWB shows a maximum capacity value higher than G3-FCC.

We point out that on equal transmitted power, the capacity improvements directly translate in range extension whenever we impose the I-UWB to achieve a rate equal to the capacity of OFDM.

We now turn our attention to the power saving that can be brought by the use of I-UWB.

In Figs. 3 and 4, we respectively show the cumulative distribution function (CDF) of the average maximum PSD level, i.e., PDS_{max} (see Section IV), required by I-UWB to

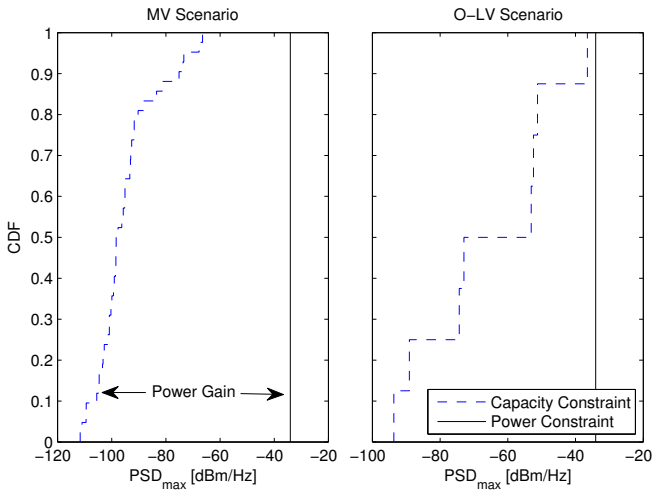

Fig. 3. CDF of the maximum value of the I-UWB average transmitted PSD (PSD_{max}) under the assumption of the same transmitted power and the same capacity of the narrow-band G3-PLC system.

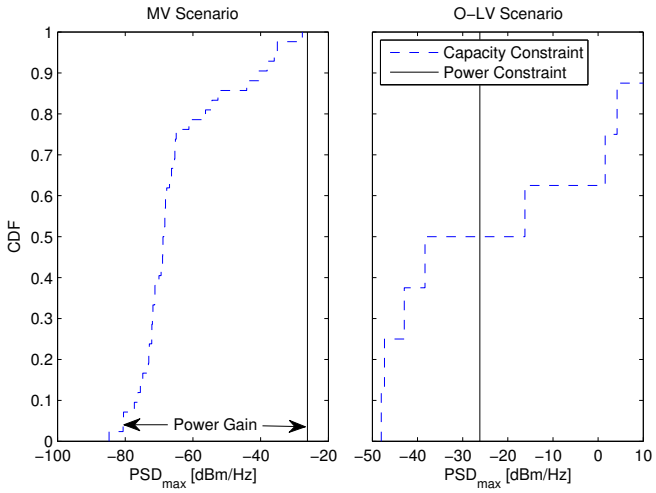

Fig. 4. CDF of the maximum value of the I-UWB average transmitted PSD (PSD_{max}) under the assumption of the same transmitted power and the same capacity of the narrow-band G3-FCC system.

achieve a target rate equal to the capacity of G3-PLC and G3-FCC. We also show the values of the PSD_{max} corresponding to the powers used by G3-PLC and G3-FCC.

From Figs. 3-4, we can make the following considerations.

- Looking at the MV scenario, with probability equal to 0.8, I-UWB achieves the same rate of G3-PLC and G3-FCC saving 43.97 and 53.82 dB, respectively.
- The power saving is still impressive considering the LV G3-PLC scenario. Nevertheless, in this case there are a 50 percent of channels where I-UWB requires more power than G3-FCC to achieves the same rate. This result clearly agrees with the fact that G3-FCC achieves higher mean capacity value than I-UWB (see Table III).

VI. Conclusions

We have proposed the use of impulsive-ultrawide band modulation for smart grid applications over distribution networks. In this respect, we have shown that I-UWB can lead to capacity improvements and power savings w.r.t. existent narrow-band OFDM based solutions, i.e., PRIME, G3-PLC, and G3-FCC.

Through numerical results, we have found that, in most cases, G3-PLC outperforms PRIME. However, both G3-PLC and PRIME are not suitable for communications over medium voltage channels. In this case, thanks to the shape of the monocycle, I-UWB is able to exploit the channel and noise characteristics. More precisely, I-UWB saves several dBs of transmitted power, still achieving the same rate of the narrow-band OFDM based solutions. This implies that, in general, it can transmit with a small average PSD level (about -80 dBm/Hz), and thus it can coexist with both narrow-band and broadband PLC devices.

References

[1] S. Galli, A. Scaglione, and Z. Wang, "For the Grid and Through the Grid: The Role of Power Line Communications in the Smart Grid," *Proc. IEEE*, vol. 99, no. 6, pp. 998–1027, May 2011.

[2] H. P. Alliance, "HomePlug Green PHY The Standard For In-Home Smart Grid Powerline Communications," 2010.

[3] P. A. T. W. Group, "Draft Standard for PoweRline Intelligent Metering Evolution R1.3E," *online at: http://www.prime-alliance.org*.

[4] ERDF, "PLC G3 Physical Layer Specification," *online at: http://www.erdfdistribution.fr/*.

[5] K. Razazian, A. Kamalizad, M. Umari, Q. Qu, V. Loginov, and M. Navid, "G3-PLC Field Trials in U.S. Distribution Grid: Initial Results and Requirements," in *Proc. of Int. Symp. on Power Line Commun. and Its App. (ISPLC)*, April 2011, pp. 153–158.

[6] Maxim, "Supplement to PLC G3 Physical Layer Specifications for Operation in the FCC Frequency Band," *online at: http://www.maxim-ic.com/*.

[7] A. M. Tonello, F. Versolatto, and C. Tornelli, "Analysis of Impulsive UWB Modulation on a Real MV Test Network," in *Proc. of Int. Symp. on Power Line Commun. and Its App. (ISPLC)*, April 2011, pp. 18–23.

[8] A. M. Tonello, R. Rinaldo, and L. Scarel, "Detection Algorithms for Wide Band Impulse Modulation Based Systems over Power Line Channels," in *Proc. of Int. Symp. on Power Line Commun. and Its App. (ISPLC)*, April 2004, pp. 367–372.

[9] M. Babic et al., "OPERA Deliverable D5. Pathloss as a Function of Frequency, Distance and Network Topology for Various LV and MV European Powerline Networks," 2005.

[10] M. Zimmermann and K. Dostert, "A Multipath Model for the Powerline Channel," *IEEE Trans. Commun.*, vol. 50, no. 4, pp. 553–559, Apr. 2002.

[11] T. Zheng, X. Yang, B. Zhang, and et al., "Statistical Analysis and Modeling of Noise on 10-kV Medium-Voltage Power Lines," *IEEE Trans. Power Del.*, vol. 22, no. 3, pp. 1433–1439, Jul. 2007.

[12] T. M. Cover and J. A. Thomas, *Elements of Information Theory*. NY: Wiley & Sons, 1991.

[13] A. M. Tonello, S. D'Alessandro, and L. Lampe, "Cyclic Prefix Design and Allocation in Bit-loaded OFDM over Power Line Communication Channels," *IEEE Trans. on Commun.*, vol. 58, no. 11, Nov. 2010.

[14] H. C. Ferreira, L. Lampe, J. Newbury, and T. G. Swart, *Power Line Communications: Theory and Applications for Narrowband and Broadband Communications over Power Lines*. NY: Wiley & Sons, 2010.

[15] N. Papandreou and T. Antonakopoulos, "Bit and Power Allocation in Constrained Multi-carrier Systems: The Single-User Case," *EURASIP J. on Advances in Signal Processing*, vol. 2008, no. Article ID 643081, 2008.

[16] A. M. Tonello, "Wideband Impulse Modulation and Receiver Algorithms for Multiuser Power Line Communications," *EURASIP Journal on Advances in Signal Processing*, vol. 2007, pp. 1–14.